A New Methodology for Assimilation of Initial Soil Moisture Fields in Weather Prediction Models Using Meteosat and NOAA Data

BART J. J. M. VAN DEN HURK

Royal Netherlands Meteorological Institute, De Bilt, the Netherlands

WIM G. M. BASTIAANSSEN AND HENK PELGRUM

DLO-Winand Staring Centre, Wageningen, the Netherlands

ERIK VAN MEIJGAARD

Royal Netherlands Meteorological Institute, De Bilt, the Netherlands

(Manuscript received 30 September 1996, in final form 3 February 1997)

ABSTRACT

In this study, a simple method is described and tested for deriving initial soil moisture fields for numerical weather prediction purposes using satellite imagery. Recently, an algorithm was developed to determine surface evaporation maps from high- and low-resolution satellite data, which does not require information on land use and synoptic data. A correction to initial soil moisture was calculated from a comparison between the evaporation fields produced by a numerical weather prediction model and the satellite algorithm. As a case study, the method was applied to the Iberian Peninsula during a 7-day period in the summer of 1994. Two series of short-term forecasts, initialized from a similar initial soil moisture field, were run in parallel: a control run in which soil moisture evolved freely and an experimental run in which soil moisture was updated daily using the simple assimilation procedure. The simple assimilation resulted in a decrease of the bias of temperature and specific humidity at 2-m height during the daytime and a small decrease of the root-mean-square error of these quantities. The results show that the surface evaporation maps, derived from the satellite data, contain a signal that may be used to assimilate soil moisture in numerical weather prediction models.

1. Introduction

Numerical weather prediction models (NWPs) perform short-term predictions of the weather on global or regional scales. In operational applications, these models are typically started a few times per day. A model run must be initialized using a reliable estimate of the actual state of the atmosphere, oceans, and land surface.

From various simulation studies, it has been shown that the performance of NWP models is partially dependent on the realism of the parameterization of subgrid-scale land-surface processes (see Garratt 1993 for a review). The exchange of water vapor and sensible heat between the land and atmosphere is to a large extent controlled by the availability of soil moisture, which has a strong feedback on vegetation development and evaporation. Soil moisture content is therefore among the most significant parameters for a reliable surface flux description (Shukla and Mintz 1982; Milly and Dunne 1994).

Most operational NWPs initialize the forecast cycle by means of a given soil moisture distribution over the forecast domain. This distribution is either obtained from a climatological database or obtained by treating the soil moisture content as a prognostic variable during the history of the forecast [e.g., the NWP of the European Centre for Medium-Range Weather Forecasts (ECMWF); see Viterbo and Beljaars 1995). The climatological database is, in most cases, a monthly averaged global map of the actual soil moisture content relative to the field capacity. A well-known database is the one prepared by Mintz and Serafini (1989, 1992). This database is derived from operational observations of precipitation and surface variables (radiation, temperature, specific humidity, and wind speed). Surface evaporation is calculated using Thornwaite's (1944) expressions.

However simple to apply, a major disadvantage of a climatological soil moisture database is its inability to adapt to anomalous conditions. After exceptionally wet (or dry) spells, the actual soil moisture content will be

Corresponding author address: Bart J. J. M. van den Hurk, Royal Netherlands Meteorological Institute, P.O. Box 201, 3730 AE De Bilt, the Netherlands.
E-mail: hurk@knmi.nl

relatively high (or low) compared to the database used. This may result in significant over- (or under-) estimations of the surface evaporation, which has a strong feedback on the predictions of cloud cover, precipitation, and low-level temperature and humidity. For instance, Moene et al. (1995) showed that the predicted occurrence of convective rainfall over the Iberian Peninsula is closely related to the soil moisture initialization.

A second disadvantage of climatological soil moisture data is the unknown accuracy of the dataset. In particular, for heterogeneous land surfaces, the significance of an average soil moisture content in an area with the typical size of an NWP grid box (say, 50 km $\times$ 50 km) is doubtful. Extreme difficulties arise when representative soil moisture content is to be determined from limited field information.

On the other hand, models treating the soil moisture content as a prognostic parameter face a major difficulty in preventing drift of the predictions. At the timescale of several weeks to several months, complex feedback loops in the model may cause a systematic over- or underestimation of the actual land-surface evaporation. As an example, the ECMWF NWP predicted a too-strong soil moisture depletion in the summer of 1994 for the entire European area, which was associated with a systematic overestimation of low-level temperature and radiation and an underestimation of precipitation and cloud cover (Viterbo 1996).

To prevent unrealistic drift, Bouttier et al. (1993a,b) present a sequential data assimilation technique, which artificially ''updates'' the model's soil moisture content by using observed model drift. This drift is expressed as differences between observed and predicted low-level temperature and atmospheric humidity. Observations are taken from operational synoptic stations. Following Mahfouf (1991), a series of statistical relationships is used to calculate soil moisture corrections in order to minimize model errors of low-level temperature and humidity. In particular, these statistical relationships depend on the land-surface parameterization scheme (in their case, the scheme of Noilhan and Planton 1989), including the treatment of vegetation and bare soil evaporation in response to ambient atmospheric conditions.

In the ECMWF model, a similar ''nudging'' is carried out, but here only the observed forecast error of the low-level specific humidity is used (Viterbo and Courtier 1995). The correction to soil moisture content is calculated as an empirical, globally constant proportionality factor times the specific humidity bias.

The sequential assimilation method implies a perfect coupling between model (errors of) low-level quantities and (errors of) initial soil moisture. A major disadvantage of the method is that model errors that are *not* related to soil moisture effects will lead to soil moisture corrections, such as miscalculations of cloud cover or effects caused by horizontal advection. In reality, the signal in the bias of near-surface temperature and humidity is only related to soil moisture under restricted conditions. No assimilation of soil moisture can be applied when horizontal advection plays a major role, or when surface fluxes are small owing to clouds, snow cover, or precipitation. A second issue of concern is the limited global coverage of surface synoptic stations, particularly in remote areas. In many areas, the reliability of the data assimilation is severely hampered by the small number of surface observations.

Bastiaanssen et al. (1997a,b) developed a methodology for estimating surface evaporation by using (cloudless) Meteosat and National Oceanographic and Atmospheric Administration (NOAA) satellite images. The algorithm is semiempirical and makes explicit use of the horizontal variability of surface temperature, surface albedo, and vegetation index. The method is also suited for high-resolution images (Pelgrum and Bastiaanssen 1996). Since soil moisture availability strongly regulates surface evaporation, a strong coupling between the horizontal distribution of the evaporation, as determined with the satellite algorithm, and the horizontal distribution of soil moisture may be expected (Bastiaanssen et al. 1997c). A case study carried out in La Mancha, Spain, during the 1991 ECHIVAL (European International Project on Climate and Hydrological Interactions between Vegetation, Atmosphere, and Land Surface) Field Experiment in Desertification-Threatened Area (EFEDA) campaign (Bolle et al. 1993) experimentally confirmed this hypothesis (Bastiaanssen et al. 1994).

The use of satellite retrievals for soil moisture assimilation will avoid some of the disadvantages of an assimilation procedure using prediction errors of near-surface parameters. The most significant advantage is that optimization of surface fluxes rather than derived near-surface state variables occurs. The surface fluxes are the variables of primary interest in the parameterization of the interaction between the land surface and atmosphere. Second, a direct observation of surface fluxes will make a soil moisture correction procedure unsensitive to the occurrence of strong horizontal advection. Finally, data coverage of satellite information is far better than synoptic data, particularly in remote areas.

In this paper, we explore the possible applicability of using evaporation maps derived from satellite data to assimilate soil moisture fields valuable for operational NWP purposes. For this, a simplified ''poor man's'' assimilation procedure is designed and tested for a single case, comprising the observed weather on the Iberian Peninsula during a 7-day period in the summer of 1994. Satellite data collected over 3 days within this period were available and were processed to evaporation maps.

The simplified soil moisture assimilation procedure is different from Mahfouf's (1991) method in that soil moisture patterns are not attributed to regional differences between measured and predicted near-surface quantities. Rather, these differences are used as a vali-

dation tool to evaluate the performance of the satellite-derived soil moisture fields. The Regional Atmospheric Climate Model (RACMO; Christensen and van Meijgaard 1992; Christensen et al. 1996) is used for the current case study.

This pilot study is designed to detect whether the satellite data contain any useful information on the land-surface energy balance. The case examined within the framework of this exercise does not represent all possible weather or land-surface types. However, it will reveal important theoretical and practical implications for a soil moisture assimilation method along these lines prior to operational implementation.

Section 2 gives a brief outline of the satellite retrieval algorithm. Section 3 describes the simple assimilation procedure and the method to verify the results. A case study and its results are described in section 4. Guidelines for further development and implementation of a similar method at a larger scale are formulated in the final section.

2. Assessment of the land-surface energy balance using satellite data

Bastiaanssen et al. (1994) and Bastiaanssen (1995) give a full description of the method for determining pixel-by-pixel evaporation rates using Meteosat and NOAA satellite imagery. The algorithm, labeled the Surface Energy Balance Algorithm for Land (SEBAL), makes explicit use of the horizontal variability of surface albedo and surface temperature, but it assumes other parameters to be constant in the domain of operation. It is therefore a *regional* algorithm, applicable to a limited area. A brief outline of SEBAL is given below.

SEBAL considers the surface energy balance equation, given by

$$Q_* = G + H + \lambda E, \quad (1)$$

in which the symbols denote the net radiation (Q_*), soil heat flux (G), sensible heat flux (H), latent heat of vaporization (λ), and evapotranspiration (E), respectively. In the current case study, SEBAL is applied to solve the surface energy balance for a series of Meteosat pixels by using Meteosat surface temperature and surface albedo, together with normalized difference vegetation index (NDVI) data obtained from the Advanced Very High Resolution Radiometer onboard the NOAA platform.

Net radiation Q_* is solved by the following steps.

- The extraterrestrial shortwave radiation is calculated as a function of the pixel wise solar zenith angle at the moment of image acquisition.
- The downward shortwave radiation at the surface K is calculated as a function of an assumed atmospheric transmittance. This transmittance is regionally constant. It may be measured in situ using a pyranometer, or derived from an atmospheric radiation transfer model.
- The surface albedo a is calculated using a simplified semiempirical radiative transfer model (Koepke et al. 1985). In this model, the surface albedo is derived from the planetary albedo, the two-way shortwave transmittance, and a correction for atmospheric reflectance, calibrated by assuming the darkest pixel in the image to have a zero surface albedo.
- An apparent atmospheric longwave emissivity is calculated using an empirical function of shortwave transmittance (Bastiaanssen 1995).
- The longwave downward radiation $L\downarrow$ is calculated by the apparent longwave emissivity and near-surface air temperature. If available, actual values of $L\downarrow$ can also be given as input.
- The Meteosat surface temperature T_s is corrected using one or more in situ observations, if available.
- The upward longwave radiation $L\uparrow$ is calculated as a function of Meteosat surface temperature and surface thermal emissivity dependent on NDVI.

The soil heat flux G is parameterized as a fraction of Q_*, following Choudhury et al. (1987):

$$\frac{G}{Q_*} = \frac{a}{100T_s}(0.32\bar{a} + 0.62\bar{a}^2)(1 - 0.98\ \mathrm{NDVI}^4), \quad (2)$$

where a is the instantaneous surface albedo, $\bar{a}$ is the surface albedo averaged over the period when the soil is heated from the sun, and T_s is the surface temperature, expressed in degrees Celsius in Eq. (2). The average surface albedo is considered to contain information on the topsoil moisture content, while T_s represents the phase lag between Q_* and G. NDVI is included to incorporate the effect of radiation extinction within a canopy layer.

For the estimation of sensible and latent heat flux, a series of steps is carried out. The first step is to assume that areas with very large evaporation rates will be recognizable as pixels with low surface albedo and relatively low surface temperature, associated with the presence of inland wetlands, storage reservoirs, shorelines, or dense vegetation stands. Areas with no evaporation will show the reverse signal—that is, relatively high surface temperature and high surface albedo. Threshold values of Meteosat albedo and surface temperature are used to define pixels with maximum evaporation equal to the available energy $Q_* - G$ (albedo $a < 0.1$ and surface temperature $T_s < 24$°C). Simultaneously, pixels with $a > 0.23$ are assumed to be associated with areas without any evaporation at all, and thus for which $H = Q_* - G$.

A scatterplot of actual Meteosat measurements of albedo and surface temperature for a heterogeneous area is shown in Fig. 1. In this figure, data for the entire Iberian Peninsula observed at noon on 1 July 1994 are displayed. Symbols shown denote average surface temperature per class of albedo values. Also plotted is a best-fit regression polynomial that shows an optimum separating an ascending and a decending branch at $a \approx$

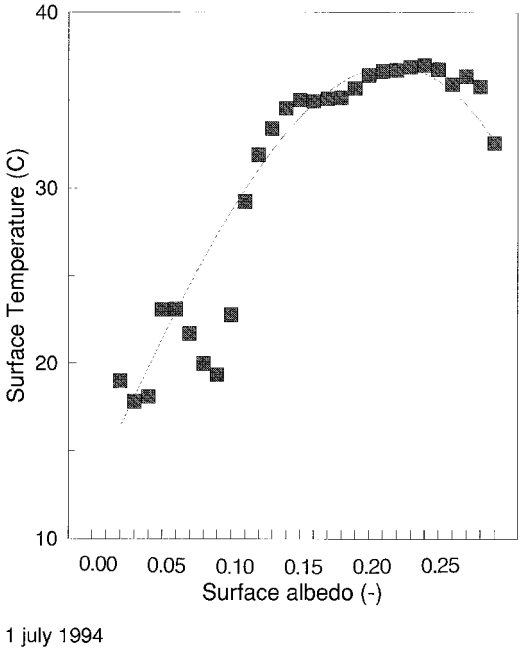

FIG. 1. Example of a scatterplot between satellite-derived surface temperature and surface albedo. Shown are Meteosat data covering the entire Iberian Peninsula on 1 July 1994.

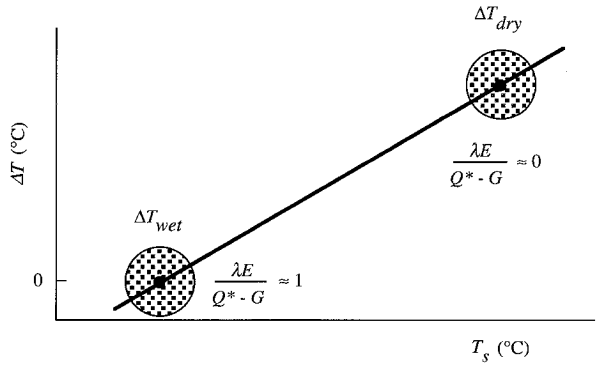

FIG. 2. Representation of the quasi-linear relationship between surface temperature T_s and temperature gradient ΔT (from Bastiaanssen 1995).

0.22. The *ascending* branch is controlled by evaporation, which leads to higher albedo and surface temperature for smaller evaporation rates. The *descending* branch represents pixels where evaporation is assumed to be negligible and shows a further decrease of T_s as the albedo increases. This branch is controlled by net radiation—increasing the surface albedo of nonevaporating land surfaces leads to a reduction of net radiation and thus of sensible heat flux. The slope of $\partial a/\partial T_s$ may be used to define a characteristic aerodynamic exchange resistance for these dry pixels, r_a^{dry} (Menenti et al. 1989). Rewriting Eq. (1) and differentiating with respect to T_s gives

$$\frac{\partial H}{\partial T_s} = -K\frac{\partial a}{\partial T_s} - \frac{\partial L^{\uparrow}}{\partial T_s} - \frac{\partial G}{\partial T_s}$$

$$= \rho c_p\left(\frac{1}{r_a^{\text{dry}}} + \Delta T^{\text{dry}}\frac{\partial}{\partial T_s}\frac{1}{r_a^{\text{dry}}}\right), \quad (3)$$

where ρ is the density of dry air and c_p the specific heat of dry air. Here, ΔT^{dry} is a characteristic vertical temperature difference for nonevaporating land surfaces in the image, defined by

$$Q_* - G = H = \rho c_p \Delta T^{\text{dry}}/r_a^{\text{dry}}. \quad (4)$$

In Eqs. (3) and (4), an implicit definition of a reference height at which the (potential) air temperature may be assumed to be identical for all dry pixel areas in the region, similar to the concept of blending height (Blyth et al. 1993), is included. This assumption puts a limit on the size of the area of operation. Here, $\partial a/\partial T_s$, $\partial L^{\uparrow}/\partial T_s$, and $\partial G/\partial T_s$ can be solved from the satellite measurement being accomplished with the semiempirical steps; ΔT^{dry} and r_a^{dry} are two unknowns, which can be found from Eq. (3) and classical flux-profile relationships. An iteration procedure is required to incorporate the effects of atmospheric stability in r_a^{dry}.

The accuracy of r_a^{dry} implicitly depends on the correlation between the surface albedo and the surface temperature of dry land-surface elements, as reflected by the radiation-controlled branch in Fig. 1. If this descending branch is clearly shaped and well defined, the resistance can be reasonably well estimated (Wang et al. 1995).

The next crucial step in SEBAL is to assume that for the entire image the relationship between the surface temperature T_s and the temperature gradient ΔT is quasi-linear (see Fig. 2). This assumption is based on field observations carried out in several (semi-) arid areas (Bastiaanssen et al. 1996). The correlation between T_s and ΔT was shown to be considerably better than the relation between T_s and the near-surface air temperature T_a (e.g., Chen et al. 1983). Then, two extreme regimes must be ''anchored'' in the image—the dry area where $\lambda E = 0$, as applied to develop Eq. (3), and a wet area where it is assumed that $\lambda E \gg H$ and so $\Delta T \sim 0$. Once the extremes are found from the regional-scale satellite image, each pixel in the image can be associated with a value of ΔT corresponding to the observed value of T_s.[1]

By use of the local terrain roughness on the basis of NDVI, together with a set of flux-profile relationships for both temperature and momentum transport, H is found for each individual pixel from ΔT; λE is the resulting term in the energy balance equation [Eq. (1)].

In the current formulation, SEBAL uses an empirical relationship to specify the roughness length for mo-

[1] Note that by this procedure T_s is used for interpolation purposes only and not used to calculate ΔT directly from a given air temperature. Hence, in situ air temperature measurements are not necessary.

mentum z_{0m} as a function of NDVI obtained from NOAA images. The roughness length for heat z_{0h} is prescribed by adopting a fixed ratio of z_{0m}/z_{0h}. The wind speed at reference height U_a is not required for each dry pixel separately since r_a^{dry} follows directly from Eq. (3). On the other hand, it is implicitly assumed that U_a is similar for all dry pixels. A reference value of 10 m s^{-1} is chosen here. An advantage of this procedure is that z_{0h}, T_s, and the air temperature are coupled correctly, and that realistic sensible heat fluxes are ensured.

The SEBAL method incorporates a series of crucial assumptions, which are all extensively discussed by Bastiaanssen (1995). In the context of using SEBAL for deriving surface evaporation maps for soil moisture initialization purposes, a few assumptions are important and worth repeating explicitly.

- The evaporation map is an instantaneous observation. Explicit use is made of the *spatial variability* within a single image, and no use is made of any *temporal* variability. The required scaling and anchoring of ΔT^{dry} are entirely based on one specific Meteosat image acquired at a single moment. This implies that the images must contain *both* pixels that represent areas with an evaporation at nearly potential scale ($H \approx 0$) *and* pixels representing areas with no evaporation at all ($\lambda E \approx 0$). Also, the radiation branch must be detectable to a minimum extent, implying that a range of dry areas with varying albedo must be captured in the image.
- The method only operates for cloud-free pixels in the image.
- There are several crucial surface parameters that must be explicitly provided—the ratio of roughness lengths for momentum and heat, atmospheric shortwave transmittance, longwave downward radiation, and an estimate of surface temperature at a number of positions for the atmospheric correction of the Meteosat thermal infrared channel.

3. Outline of a poor man's assimilation procedure

a. Basic assimilation steps

Assuming that the evaporative fraction Λ, defined as $\lambda E/(H + \lambda E)$ and derived by SEBAL, is realistic, we can adjust Λ, as calculated by the NWP model by varying the initial soil moisture content ω in the NWP; Λ is a convenient comparison parameter since it is a surface wetness indicator, which is normalized by the available energy $Q_* - G$. It shows a fairly constant value during daytime, between about 1000 and 1400 UTC, and as such its temporal stability is better than λE or the resistance to evaporation. Insensitivity to temporal variability is necessary when SEBAL and the NWP are not synchronized. The purpose of the assimilation method is to define for each NWP grid point a value of ω that minimizes $|\Lambda_{\text{NWP}} - \Lambda_{\text{SEBAL}}|$, where the latter quantity is a simple averaged evaporative fraction of all valid Meteosat pixels located within the NWP grid box (see below).

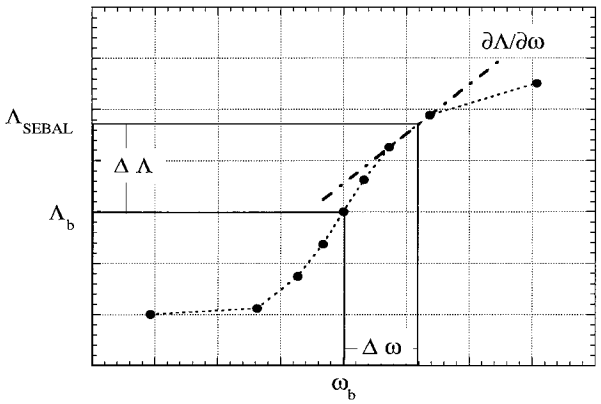

FIG. 3. Graphic representation of the poor man's assimilation method. Shown are the linear relationships between ω and Λ, as predicted by the NWP model, and the simple regression method for obtaining an optimal soil moisture content given Λ, as derived from SEBAL.

The NWP model used here, RACMO, is a limited-area numerical weather prediction model (Christensen and van Meijgaard 1992). The physical package of RACMO is basically inspired on the climate model of the Max Planck Institute (ECHAM) and as such provides a sophisticated tool for research purposes.

As a surface boundary condition over land, RACMO includes a single-layer soil hydrology scheme (Dümenil and Todini 1992). Therefore, only one parameter (the moisture content in the soil moisture volume) needs to be adjusted to minimize $\Lambda_{\text{SEBAL}} - \Lambda_{\text{RACMO}}$; Λ_{RACMO} is the value of Λ found by initialization using a background soil moisture content ω_b. This background value can be a climatological value or the first guess resulting from a previous run with the NWP model.

In the simplified assimilation method, a correction to ω_b was found by assuming a quasi-linear relationship between ω and Λ. This relationship was assessed by executing a set of runs with RACMO, which only differed with respect to the amount of initial soil moisture. Then, the correction to ω_b, identified as $\Delta\omega$, was found from $\Delta\Lambda$ (the difference between Λ_{RACMO} and Λ_{SEBAL} using a simple linear regression (see Fig. 3).

$$\Delta\omega = \omega_i + \frac{\omega_j - \omega_i}{\Lambda_j - \Lambda_i}(\Lambda_{\text{SEBAL}} - \Lambda_i) - \omega_b, \qquad (5)$$

where subscripts i and j refer to RACMO runs for which Λ is closest to Λ_{SEBAL}. Any nonlinear sensitivity $\partial\Lambda/\partial\omega$ within the range ω_i to ω_j is ignored.

For the current study, 12 runs of RACMO were carried out. In addition to the background run, 9 runs were executed in which initial soil moisture was varied be-

tween 35% and 75% saturation at intervals of 5%.[2] Furthermore, one ''wet'' run (100% saturation) and one ''dry'' run (10% of the July climatology derived from Mintz and Serafini 1992) were carried out. As a ''cold start'' on the first day, the July climatology was used as the background run.

Both SEBAL and NWP evaporative fractions were derived for 1200 UTC, when surface fluxes are strong. The NWP fields were generated from a 12-h forecast started at 0000 UTC, with soil moisture fields initialized as indicated above.

SEBAL calculates evaporative fractions on the Meteosat pixel scale, which is at a much finer scale than the RACMO grid, with a typical size of 50 km $\times$ 50 km. For purpose of simplicity, the SEBAL fluxes calculated at all pixels within a single RACMO grid box were averaged. Then, Λ_{SEBAL} was calculated from these average fluxes according to

$$\Lambda_{\text{SEBAL}} = \bar{\Lambda} = \frac{\sum_{i=1}^{n} \lambda E_i}{\sum_{i=1}^{n} (\lambda E_i + H_i)}, \qquad (6)$$

where the summation is over all Meteosat pixels *i* within an NWP grid box. Cloudy pixels were excluded from the averaging. Typically, for the current case study, approximately 70 SEBAL pixels were averaged to a single RACMO grid-box value.

b. Verification of results

In contrast to the methods described by Bouttier et al. (1993a) and Viterbo and Courtier (1995), low-level synoptic-observations of temperature and specific humidity are not used as sources of information for obtaining a new initial soil moisture field. Therefore, the routinely available data can be used as independent verification material to evaluate the performance of the assimilation procedure.

In the current study, we carried out a series of 42-h runs with RACMO, with soil moisture initialized as described above. In the current setup, operational ECMWF analyses are used as boundary data. All runs are started at initial time t = 0000 UTC. The results of the simulation period between t + 24 h and t + 42 h are evaluated. The choice for this evaluation interval is somewhat arbitrary, but it allows the model to adjust the lowest atmospheric layers to the change in the land-surface boundary conditions. Simultaneously, it is considered to be still short enough to avoid too-large discrepancies from real-time large-scale weather phenomena.

We express model results as an average bias and root-mean-square (rms) error of an ensemble of synoptic observations of temperature and specific humidity at 2-m height in a selected area. The 2-m quantities in RACMO are calculated from model variables by an interpolation between the surface and the lowest model level following Monin–Obukhov theory (Geleyn 1988). The horizontal interpolation to synops station coordinates is carried out using a simple bilinear interpolation (see section 4 for more details).

4. Selected case study and results

a. Selected case study

For the current case study, a 7-day period in 1994 (1–7 July) was selected for the Iberian Peninsula, which was a relatively dry summer. The Iberian weather was characterized as cloud-free and warm (the temperature at 2 m was approximately 35°C in central Spain), with weak winds from westerly directions. The selection of the case study was based on the following arguments.

- The SEBAL algorithm requires a series of extreme surface conditions in terms of the surface evaporation. Also, cloud cover during the period was limited.
- The impact of soil moisture on atmospheric quantities is particularly present under conditions in which the surface receives enough energy to evaporate or heat the air. Wintertime or nighttime conditions are therefore less relevant for the issue of soil moisture initialization.
- An expected benefit of assimilation of soil moisture using available data is the improvement of the regional distribution of soil moisture and its impact on predicted atmospheric quantities. The case study is preferably situated in an area with significant horizontal gradients. The Iberian Peninsula shows a strong gradient in soil moisture climatology—wet in the northwest and rather dry in the central and southeastern part of Spain (see Figure 4).
- For reasons of practical origin, the case study could only be carried out for a limited area and period of time. SEBAL results were generated for 1, 5, and 7 July 1994 only.
- During the selected period, ground flux measurements, collected in the context of the EFEDA-II campaign (Bolle et al. 1993), were available. Ogink-Hendriks et al. (1995) showed field data of Λ collected in the vicinity of the city of Tomelloso, La Mancha, Spain. A brief validation of SEBAL results for Λ using these data is shown below.

The data used to validate the runs with the new soil moisture field are taken from operational synops stations, extracted from the ECMWF Meteorological Ar-

[2] These limits represent the range in which the land-surface evaporation parameterization in RACMO shows a significant response to ω. The lowest value may be interpreted as the wilting point, while the higher value represents field capacity.

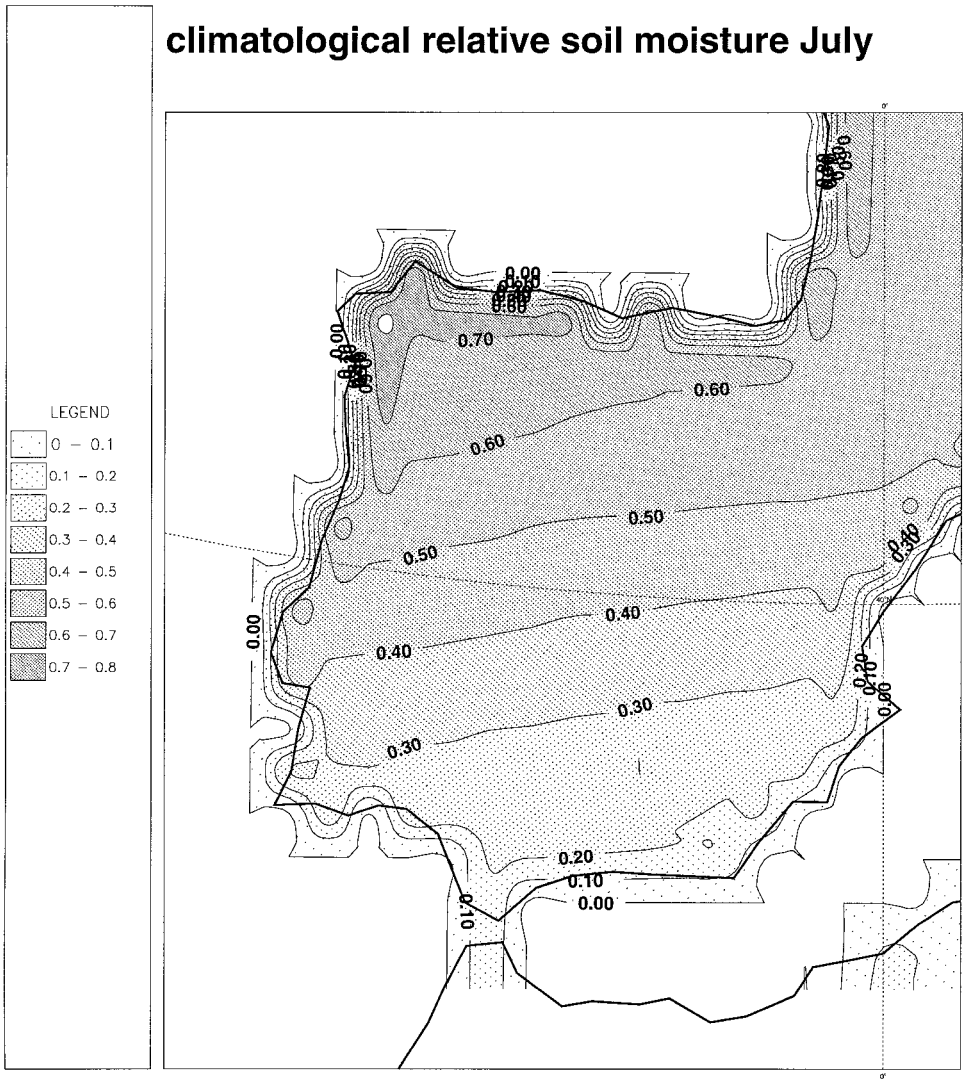

FIG. 4. Climatological soil moisture field for the Iberian Peninsula for July, as used by RACMO operationally. Shown is the fraction of soil moisture saturation, defined as ω/ω_{sat}, with ω_{sat} being the maximum soil moisture content (after Mintz and Serafini 1989).

chival and Retrieval System (MARS). In MARS, synoptic data are available at 6-h time intervals. Stations at coordinates for which the fraction of the model grid box covered by land did not exceed 0.7 were excluded. Also stations for which the difference between the height of the station and the average height of the grid box interpolated to the station coordinate exceeded 300 m were excluded from the analysis (Navascues 1996). These criteria are rather arbitrary, but exclude large biases owing to a poor representativity of the synoptic information. The filtering retained approximately 35 stations for the final intercomparison. The number of comparison data points varies per time slot and per parameter since the data submission is not always identical.

b. Verification of SEBAL results with ground-based flux measurements

In the context of the EFEDA-II campaign (Bolle et al. 1993), eddy correlation measurements of sensible and latent heat flux were conducted in an extensive vineyard near Tomelloso, Spain, during June and July 1994 (see also van den Hurk 1996). Three SEBAL Λ maps were constructed in this period for 1, 5, and 7 July 1994, around solar noon. Measured values of Λ are shown in Fig. 5, together with SEBAL estimates at selected times. A reasonable agreement is shown, but the data presented in Fig. 5 have to be interpreted carefully. Field measurements of eddy correlation fluxes represent a footprint of approximately 1 km^2 in size. Since Meteosat

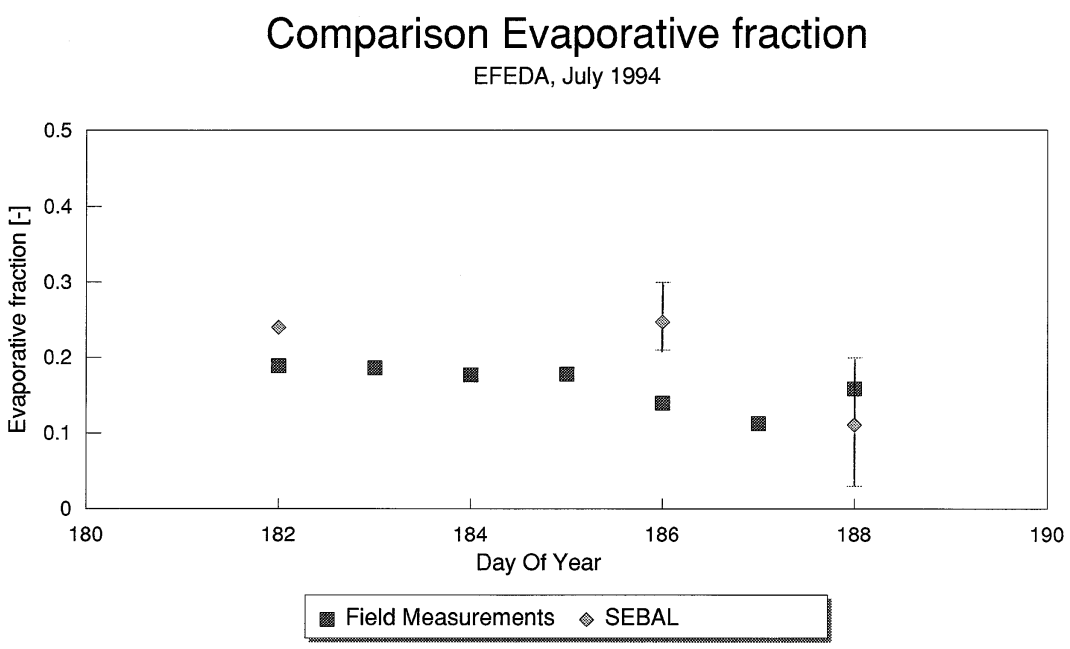

FIG. 5. Evaporative fraction Λ measured at a vineyard site in La Mancha during 1–7 July 1994. Shown are eddy correlation averages between 1000 and 1400 UTC (squares), and instantaneous SEBAL estimates at noon for 3 days (diamonds). Error bars represent standard deviation values for nine neighboring Meteosat pixels, centered at the field measurement location.

pixels are sampled at a coarser resolution, even a single pixel cannot directly be compared to field data. This discrepancy of scales can only be bridged by inclusion of another scale of information, that of high-resolution imagery. For instance, Landsat Thematic Mapper data can encompass both the in situ flux measurements and the Meteosat pixel size. In spite of the scale difficulties, the weekly averaged value of Λ appeared to be 0.2 for SEBAL and 0.16 for the field measurements, which is a fair agreement.

c. Construction of a new soil moisture field

Soil moisture corrections were calculated as indicated by Eq. (5) for 3 days (1, 5, and 7 July 1994). Grid values for which no soil moisture update was available (either because of excessive cloud cover in both SEBAL maps, or because of their lying outside the SEBAL domain) were kept at the previous background value. The background soil moisture field for generating a new soil moisture map for 1 July was derived from the Mintz and Serafini database. Figure 6 shows the new initial soil moisture map for the Iberian Peninsula for 1 July 1994, which is to be compared with the climatological field (Fig. 4).

It is clearly seen from an intercomparison between Figs. 4 and 6 that the the new soil moisture fields gives *higher* soil moisture values in central and most of southern Spain. In spite of the fact that 1994 was a relatively dry summer for the European continent (Viterbo 1996), the SEBAL algorithm suggested that local climatology is too dry for that particular period. On the other hand, a clear *reduction* of soil moisture is enforced in the area east of Madrid, Spain, as well as near the northeast border of Portugal. A pronounced redistribution of soil moisture results from this simple assimilation method. On average, the initial soil moisture increased by approximately 20% relative to the climatological value.

Another clear aspect from Fig. 6 is the increased amount of detail in the soil moisture fields. Rather localized features are visible, in contrast to the climatological field.

Figure 7 shows a frequency distribution of the evaporative fraction for Iberian NWP grid boxes, valid for 1200 UTC 1 July 1994. Apart from SEBAL data, results from RACMO after 12 h of simulation, initialized using the soil moisture field of Fig. 6, are shown. The correspondence between the two distributions is very good, although RACMO tends to give slightly lower evaporative fractions. This may well be a result of the assumed linearity of $\partial\Lambda/\partial\omega$ within the chosen 5% intervals of ω. For comparison, a RACMO run initialized from the Mintz and Serafini climatology (Fig. 4) is also shown, revealing a large number of grid boxes for which surface evaporation is far too low.

Two parallel series of 42-h forecast runs were started daily at 0000 UTC, between 1 and 7 July 1994. For

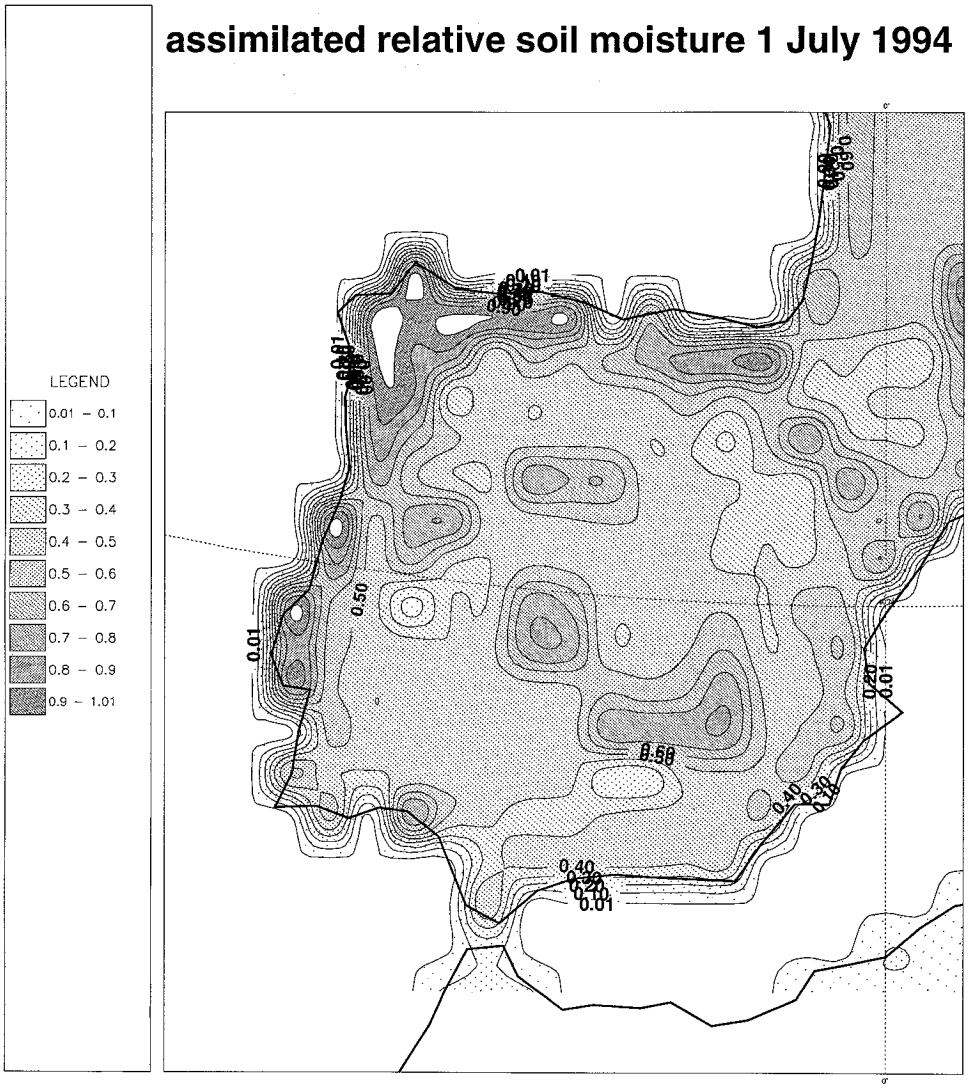

FIG. 6. New soil moisture field obtained using the simple assimilation procedure (see text). Shown are relative soil moisture contents, similar to those in Fig. 4.

both series, the assimilated soil moisture field obtained for 1 July 1994 was used as the initial condition. In the first series, the *control* runs, soil moisture was not adjusted further and was treated as an unanalyzed prognostic parameter during the remaining days. From 2 July onward, initial soil moisture was obtained from the $t + 24$ run started the day before.

In the second series, labeled the *experimental* runs, a daily adjustment of soil moisture was carried out. For 5 and 7 July, the available soil moisture fields were used for this purpose. For intermediate days, a simple linear interpolation between the available data was carried out to ensure a gradual relaxation to a new set of soil moisture data. This interpolation was carried out in order to mimic the effect of a daily input of satellite data, which might be expected in a routine data assimilation cycle.

d. Results of simulations with the new initial soil moisture field

Figure 8 shows the Iberian averages of soil moisture (lower panel) and the evaporative fraction (upper panel) for SEBAL and the two RACMO runs. SEBAL soil moisture is displayed at initialization time (0000 UTC), while the RACMO results are shown at noon, after 12 h of simulation. The combination of SEBAL data and RACMO runs shows a significant increase of soil moisture between 1 and 5 July, and a slight decrease after this period. Since no precipitation was simulated in the RACMO runs, the soil moisture content in the control runs continues to decrease during this 7-day period. As a result, the evaporative fraction of the experimental runs is considerably higher than that in the control runs and follows the SEBAL data closely at times where this is available.

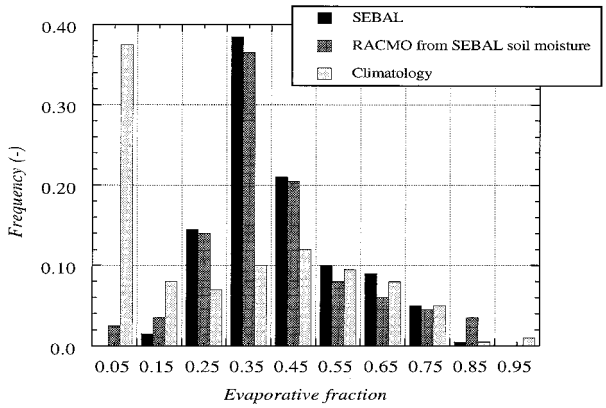

FIG. 7. Frequency distribution of evaporative fraction valid on 1200 UTC 1 July 1994. Shown are distributions of SEBAL data (dark bars) and results from RACMO after 12 h of simulation, started from a climatological soil moisture field (light bars) and from a soil moisture field derived from regression between multiple RACMO runs (shaded bars).

The apparent *increase* of soil moisture between 1 and 5 July, as derived from the SEBAL estimates of Λ, cannot be explained in terms of synoptic events, such as rainfall or excessive dew. It is most likely an artifact of the assumed perfect coupling between soil moisture and the evaporative fraction. In reality, other factors will likely have contributed to an apparent increase of Λ, as calculated using SEBAL. Note, however, that the calculated evaporative fraction from RACMO responds nonuniformly to the gradual change of ω; after 3 July, a sharp decrease of Λ is simulated for both RACMO runs, in spite of the lack of a quick change of imposed initial soil moisture. A change of the atmospheric circulation is likely causing the sudden decrease of land-surface evaporation.

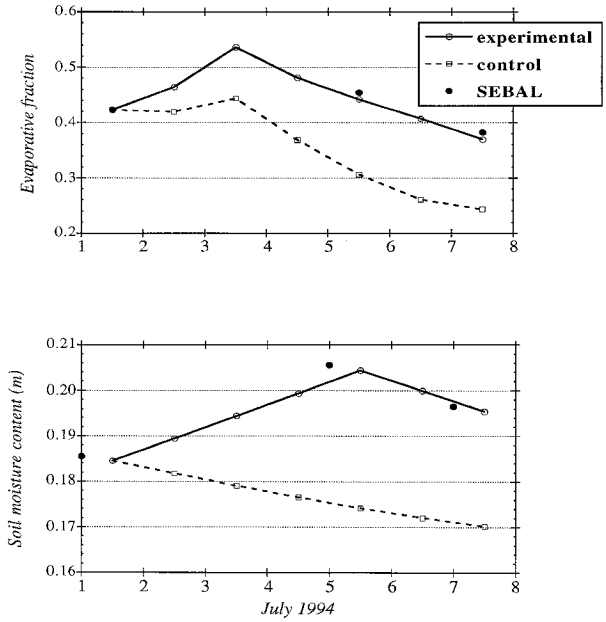

FIG. 8. Upper panel: average evaporative fraction at noon for Iberian grid points, calculated by SEBAL (symbols) and RACMO after 12 h of simulation; solid lines represent the experimental runs with daily adjustment of soil moisture, while dashed lines represent the control runs without soil moisture adjustment. Lower panel: average soil moisture content for the same cases. SEBAL results are shown at initialization time, while RACMO results are shown after 12 h of simulation.

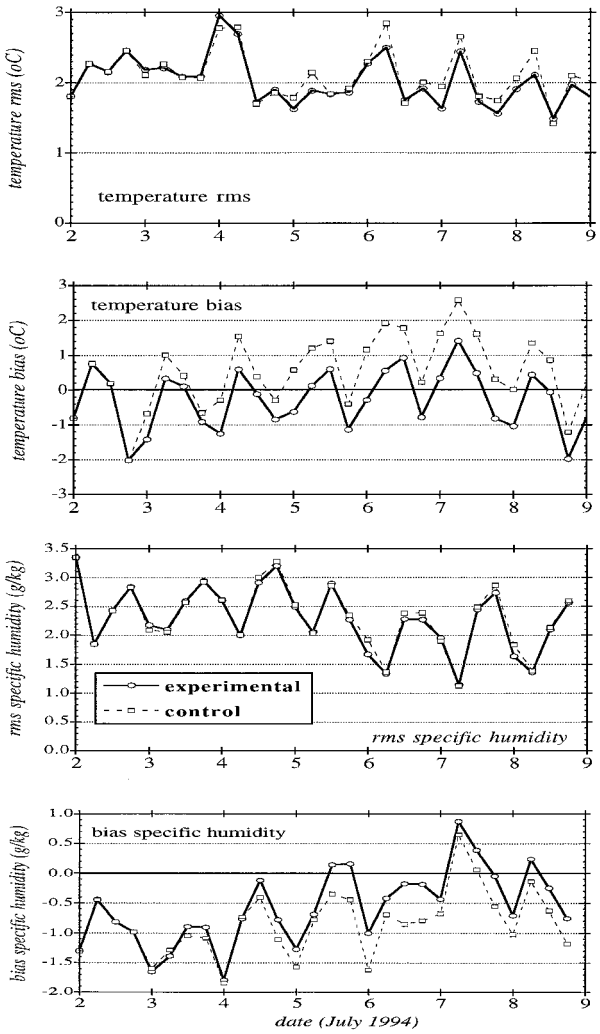

FIG. 9. Bias and root-mean-square error of 2-m temperature (upper panels) and 2-m specific humidity (lower panels). Shown are the model performances using the control run without soil moisture adjustment (dashed lines) and the experimental runs with daily adjustment (solid lines). The time indicated is the evaluation time. Shown are simulations from $t + 24$ h (0000 UTC) to $t + 42$ h (1800 UTC).

Figure 9 shows the bias and rms (corrected for bias) of the model performance in terms of 2-m temperature (upper panels) and 2-m specific humidity (lower panels). Both the control runs and the experimental runs with daily updated initial soil moisture are shown. The time shown is the verification time, achieved after 24–42 h of model simulation. Results for 2 July (0000–1800 UTC) are identical for both series of runs.

Concentrating on the bias of the 2-m temperature, a clear diurnal variation is evident. For the experimental runs, the bias signal remains similar for all simulation days and is typically −1.5°C for late afternoon and midnight, and 0°–1°C for early morning and noon. The control run shows a systematic increase of the bias of 2-m temperature. The difference between the two series of runs exceeds 1°C by the end of the simulation week.

An opposite signal is present in the average specific humidity bias. A systematic underestimation of the near-surface specific humidity of approximately 1 g kg^{-1} is shown early in the simulation period. In the generally wetter experimental runs, this underestimation is slightly removed, while the control runs continue to show a systematic negative specific humidity bias.

In all cases, the bias is smaller during daytime than during nighttime. During daytime, the interaction between the surface and the lowest atmospheric levels is strong since surface heat fluxes are generally large. During nighttime, a much weaker coupling between soil moisture and low-level atmospheric quantities exists, and the change of the model predictions of near-surface quantities must be a result of the change of the entire boundary layer during daytime.

A modest improvement of the experimental runs as opposed to the control is also visible in the rms error of 2-m temperature, which is up to 0.3°C lower. The reduction of rms implies that the change of the geographic distribution of soil moisture has a beneficial impact on the geographic distribution of calculated surface fluxes. Hardly any impact is visible in the rms error of near-surface specific humidity. The impact of the simulations on the rms errors is sincerely concealed by the relatively small sample size, not exceeding 35 stations during daytime and approximately 15 at midnight.

5. Conclusions and guidelines for further development

The results presented here reveal that, under the specified test conditions, some significant information is present in the SEBAL evaporative fraction fields that is compatible with information on forecast errors provided by synoptic observations. It is of particular importance to note that the *sign* of the SEBAL signal is compatible to what is found from the synoptic observations—an average underestimation of Λ in the control runs is detected by both SEBAL (yielding higher Λ) and the synoptic data (confirming on an underestimation of Λ by showing that the model gives a too-low specific humidity and a too-high temperature during daytime).

The SEBAL signal appears to be strong enough to correct for an underestimation of land-surface evaporation within the time course of only a week. Whether this underestimation of Λ by the control run is a result of model drift or caused by other effects (such as a bias in the analysis of atmospheric fields or sudden synoptic events not anticipated by the model) is not clear.

The first results from the feasibility study presented in this paper are rather encouraging in the context of using Meteosat and NOAA data for assimilation of soil moisture fields. However, some scientific and practical issues need further attention prior to the operational use of a retrieval algorithm along the lines of SEBAL for soil moisture initialization.

The most intriguing matter to be resolved is whether SEBAL will also give reliable results under conditions that differ from the semiarid circumstances explored in the test case. As commented before, SEBAL is expected to work relatively well in these areas since the assumption of the presence of both very dry and very wet pixels is met during most of the summer season here.[3] However, NWP models cover a much wider range of climate zones, and it is important that the assimilation scheme shows proper behavior in the entire simulation area. It must be verified that the assimilation procedure derived from the SEBAL algorithm can be applied in the whole of Europe. Special attention must be paid to the following factors.

- The performance of SEBAL in other seasons than full summer—the strongest changes of soil moisture in Europe occur generally in spring, as the growing season starts and evaporation becomes stronger, and model drifts often originate in this period (Viterbo 1996), so a proper control of these drifts is of major practical importance;
- The role of the soil moisture parameterization in model drift in temperate climate regions;[4]
- Situations of long periods of cloud cover in certain areas, which might play a role in some of the northern and western European areas in early and late summer; and
- The treatment of NWP grid boxes that are only partially covered with land surface.

A second major issue is to improve the compatibility of the satellite retrieval system and the NWP environment. For the purpose of this feasibility study, SEBAL and RACMO were operated fully independently from each other. This implies that differences are present in the distribution of, for instance, surface albedo, roughness, soil heat flow, and even vegetation cover. In a future study, methodological incompatibilities must be minimized as much as possible by sharing datasets of this nature where possible.

Related to this issue, a possible route for improving the quality of SEBAL-generated Λ fields is to force the algorithm with analyzed wind fields at reference height,

[3] SEBAL is also expected to work rather well under conditions of intermittent precipitation, where the full benefit of the regional differentiation by SEBAL is foreseen.

[4] With respect to this issue, a study is planned in which the performance of SEBAL is evaluated using synoptic and field data collected near Cabauw, the Netherlands.

rather than estimating it from r_a^{dry}, as was explained in Eq. (3). Preliminary attempts have shown only a modest sensitivity of Λ to this adjustment, justifying the crude approximation carried out in this study. However, a more systematic investigation is to be carried out, particularly for weather situations with strong horizontal wind gradients.

Probably of more significance is the need to replace the parameterization of incoming longwave radiation by analyzed fields. It is not clear how the parameterization of $L\downarrow$ adopted here has affected the values of Λ calculated by SEBAL.

Third, the surface scheme in RACMO is provided with only a single soil layer. However, as is shown by Viterbo (1996), moisture in the deep soil layers has a relatively long variation timescale, as opposed to near-surface soil moisture, which can show considerable diurnal variations. It is expected that an improvement of the assimilation scheme can be obtained when the soil moisture increments are divided over surface and deeper layers by making use of the available vegetation cover degree, as specified in the NWP explicitly. Under conditions with large portions of bare soils, a mismatch in Λ between SEBAL and RACMO will lead to a correction of the moisture content in the top soil layer—that is, bare soil evaporation will dominate over canopy evaporation. For large canopy covers, more weight will be paid to the correction of deeper soil moisture contents controlled by canopy evaporation. This mechanism allows for a distinction between long-term drift (induced by errors in the deep reservoir) and short-term errors, which are more likely to be caused by errors of, for instance, predicted precipitation distributions.

This distinction between deep and surface soil moisture reservoirs is important in the context of preventing NWP models from drifting. The drift of the land-surface moisture content is in fact a result of an accumulation of model errors from the past into the soil reservoir, amplified by model feedback mechanisms. This type of drift has a relatively long timescale, on the order of up to 4 months (Betts et al. 1996). This timescale consideration has as the practical implication that a correction of the soil moisture content using available field information does not have to be carried out daily, but will probably be sufficient when employed a few times per month. This relaxes the constraint that the use of SEBAL requires the occurrence of cloud-free conditions in a given area.

A more practical matter of concern is the overwhelming demanding for computer resources to perform a series of typically 12 complete (12 h) simulation runs, only to generate an initial soil moisture field in an operational environment. It is more practical to incorporate the soil moisture initialization in an operational data assimilation system, where a short-term simulation and all available data are blended into an initial model state. With respect to the soil moisture assimilation, the simplest solution is to construct an extensive database of sensitivity functions $\partial\omega/\partial\Lambda$, representative for a large range of land-surface and atmospheric conditions, using a single-column formulation of the NWP model. Simple optimum interpolation techniques can be used to define soil moisture corrections for a specified set of conditions, including information on estimated observation errors (Daley 1991).

Acknowledgments. This study was made possible by the BCRS-EOS Bridging Phase Programme. Special acknowledgments are given to Anton Beljaars, who initiated much of the present work at KNMI and ECMWF, and to Massimo Menenti for taking the leading role in the BCRS-EOS project. Also, additional input by Bert Holtslag is greatly appreciated, and the authors acknowledge the illuminating discussions carried out with colleagues at ECMWF and KNMI, particularly Pedro Viterbo, Jean-Francois Mahfouf, Gerard Cats, Ben Wichers Schreur, and Toon Moene. Three anonymous reviewers showed much interest and offered useful suggestions for improvement of the analysis and the manuscript.

In situ surface flux measurements were carried out under auspices of Pavel Kabat, and analyzed and made available by Marja Ogink-Hendriks at SC-DLO. We are indebted to them for their assistance and also that of other EFEDA-II members.

REFERENCES

Bastiaanssen, W. G. M., 1995: Regionalization of surface flux densities and moisture indicators in composite terrain—A remote sensing approach under clear skies in Mediterranean climates. Ph.D. thesis, Agricultural University, 273 pp. [Available from DLO-Staring Centre, P.O. Box 125, 6700 AE Wageningen, the Netherlands.]

——, D. H. Hoekman, and R. A. Roebeling, 1994: A methodology for the assessment of surface resistance and soil water storage variability at mesoscale based on remote sensing measurements: A case sudy with HAPEX-EFEDA data. IAHS Special Publication 2, IAHS Press, Oxfordshire, United Kingdom, 66 pp. [Available from DLO-Staring Centre, P.O. Box 125, 6700 AE Wageningen, the Netherlands.]

——, M. Menenti, A. J. Dolman, R. A. Feddes, and H. Pelgrum, 1996: Remote sensing parameterization of meso-scale land surface evaporation. *Radiation and Water in the Climate System: Remote Sensing Measurements,* E. Raschke, Ed., NATO ASI Series, Vol. I.45, Springer-Verlag, 401–429.

——, ——, R. A. Feddes, and A. A. M. Holtsag, 1997a: A remote sensing surface energy balance algorithm for land (SEBAL). Part 1: Formulation. *J. Hydrol.,* in press.

——, H. Pelgrum, J. Wang, Y. Ma, J. F. Moreno, G. J. Roerink, R. A. Roebeling, and T. van der Wal, 1997b: A remote sensing surface energy balance algorithm for land (SEBAL). Part 2: Validation. *J. Hydrol,* in press.

——, H. Pelgrum, P. Droogers, H. A. R. de Bruin, and M. Menenti, 1997c: Area-average estimates of evaporation, wetness indicators and top soil moisture during two golden days in EFEDA. *Agric. For. Meteor.,* in press.

Betts, A. K., J. H. Ball, A. C. M. Beljaars, M. J. Miller, and P. Viterbo, 1996: The land surface-atmosphere interaction: A review based on observational and global modeling perspectives. *J. Geophys. Res.,* **101**(D3), 7209–7225.

Blyth, E. M., A. J. Dolman, and N. Wood, 1993: Effective resistance

to sensible and latent heat flux in heterogeneous terrain. *Quart. J. Roy. Meteor. Soc.*, **119,** 423–442.

Bolle, H.-J., and Coauthors, 1993: EFEDA: European Field Experiment in a Desertification-Threatened Area. *Ann. Geophys.*, **11,** 173–189.

Bouttier, F., J.-F. Mahfouf, and J. Noilhan, 1993a: Sequential assimilation of soil moisture from atmospheric low-level parameters. Part I: Sensitivity and calibration studies. *J. Appl. Meteor.*, **32,** 1335–1351.

——, ——, and ——, 1993b: Sequential assimilation of soil moisture from atmospheric low-level parameters. Part II: Implementation in a mesoscale model. *J. Appl. Meteor.*, **32,** 1352–1364.

Chen, E., L. H. Allen, J. F. Bartholic, and J. F. Gerber, 1983: Comparison of winter-nocturnal geostationary satellite infrared-surface temperature with shelter-height temperature in Florida. *Remote Sens. Environ.*, **13,** 313–327.

Choudhury, B. J., S. B. Idso, and R. J. Reginato, 1987: Analysis of an empirical model for soil heat flux under a growing wheat crop for estimating evaporation by an infra-red temperature based energy balance equation. *Agric. For. Meteor.*, **39,** 283–297.

Christensen, J. H., and E. van Meijgaard, 1992: On the construction of a regional atmospheric climate model. KNMI Scientific Rep. 147, 22 pp. [Available from KNMI, P.O. Box 201, 3730 AE De Bilt, the Netherlands.]

——, O. B. Christensen, P. Lopez, E. van Meijgaard, and M. Botzet, 1996: The HIRHAM4 Regional Atmospheric Climate Model. Scientific Rep. 96-4, Danish Meteorological Institute, Copenhagen, Denmark, 51 pp. [Available from KNMI, P.O. Box 201, 3730 AE De Bilt, the Netherlands.]

Daley, R., 1991: *Atmospheric Data Analysis.* Cambridge University Press, 457 pp.

Dümenil, L., and E. Todini, 1992: A rainfall-runoff scheme for use in the Hamburg climate model. *Advances in Theoretical Hydrology,* J. P. O'Kane, Ed., European Geophysical Society Series on Hydrological Sciences, Vol. 1, Elsevier Science Publishers, 129–157.

Garratt, J. R., 1993: Sensitivity of climate simulations to land-surface and atmospheric boundary-layer treatments: A review. *J. Climate,* **6,** 419–449.

Geleyn, J. F., 1988: Interpolation of wind, temperature and humidity values from model levels to the height of measurements. *Tellus,* **40A,** 347–351.

Koepke, P., K. T. Kriebel, and B. Dietrich, 1985: The effect of surface reflection and of atmospheric parameters on the shortwave radiation budget. *Adv. Space Res.*, **5,** 351–354.

Mahfouf, J.-F., 1991: Analysis of soil moisture from near-surface parameters: A feasibility study. *J. Appl. Meteor.*, **30,** 1534–1547.

Menenti, M., W. G. M. Bastiaanssen, D. van Eick, and M. H. Abd El Karim, 1989: Linear relationships between surface reflectance and temperature and their application to map actual evaporation of groundwater. *Adv. Space Res.*, **9,** 165–176.

Milly, P. C. D., and K. A. Dunne, 1994: Sensitivity of the global water cycle to the water-holding capacity of land. *J. Climate,* **7,** 506–526.

Mintz, Y., and Y. V. Serafini, 1989: Global climatology of soil moisture and water balance. LMD Note 148, Laboratoire de Météorologique Dynamique du CNRS, Paris, France.

——, and ——, 1992: A global climatology of soil moisture and water balance. *Climate Dyn.*, **8,** 13–27.

Moene, A. F., H. A. R. de Bruin, and A. A. M. Holtslag, 1995: Validation of the surface parametrization of HIRLAM using surface-based measurements and remote sensing data. KNMI Scientific Rep. WR 95-07, KNMI, De Bilt, the Netherlands, 45 pp. [Available from KNMI, P.O. Box 201, 3730 AE De Bilt, the Netherlands.]

Navascues, B., 1996: Analysis of 2m temperature and specific humidity. *Proc. HIRLAM 3 Workshop on Soil Processes and Soil/Surface Data Assimilation,* Madrid, Spain, SMHI/INM, 38–44.

Noilhan, J., and S. Planton, 1989: A simple parametrization of land surface processes for meteorological models. *Mon. Wea. Rev.*, **117,** 536–549.

Ogink-Hendriks, M. J., P. Kabat, J. A. Elbers, W. G. M. Bastiaanssen, and H. G. M. van der Elsen, 1995: Contribution to the EFEDA field campaigns in 1991 and 1994. Rep. 112, DLO-Winand Staring Centre, Wageningen, the Netherlands, 150 pp. [Available from DLO-Staring Centre, P.O. Box 125, 6700 AE Wageningen, the Netherlands.]

Pelgrum, H., and W. G. M. Bastiaanssen, 1996: An intercomparison of techniques to determine the area-averaged latent heat flux from individual in situ observations: A remote sensing approach using the European Field Experiment in a Desertification-Threatened Area data. *Water Resour. Res.*, **32,** 2775–2786.

Shukla, J., and Y. Mintz, 1982: Influence of land surface evapotranspiration on the earth's climate. *Science,* **215,** 1498–1501.

Thornwaite, C. W., 1944: Report of the Committee on Transpiration and Evaporation. *Trans. Amer. Geophys. Union,* **25,** 683–693.

van den Hurk, B. J. J. M., 1996: Sparce canopy parameterizations for meteorological models. Ph.D. thesis, Wageningen Agricultural University, 272 pp. [Available from Dept. of Meteorology, Duivendaal 2, 6701 AP Wageningen, the Netherlands.]

Viterbo, P., 1996: The representation of surface processes in general circulation models. Ph.D. thesis, University of Lisbon, 201 pp. [Available from ECMWF, Shinfield Park, Reading R62 GAX, United Kingdom.]

——, and A. C. M. Beljaars, 1995: An improved land surface parametrization scheme in the ECMWF model and its validation. *J. Climate,* **8,** 2716–2748.

——, and P. Courtier, 1995: The importance of soil water for medium-range weather forecasting. Implications for data assimilation. *Proc. WMO Workshop on Imbalances of Slowly Varying Components of Predictable Atmospheric Motions,* Beijing, China, World Meteor. Org., 121–130.

Wang, J., Y. Ma, M. Menenti, W. G. M. Bastiaanssen, and Y. Mitsuta, 1995: The scaling-up of processes in the heterogeneous landscape of HEIFE with the aid of satellite remote sensing. *J. Meteor. Soc. Japan,* **73,** 1235–1244.